Characterization of Bodipy Dimers Formed in a Molecularly Confined Environment

Dina Tleugabulova, Zheng Zhang, and John D. Brennan*

Department of Chemistry, McMaster University, Hamilton, ON, L8S 4M1 Canada

Received: October 3, 2002

Recently, Johansson and co-workers provided the first direct evidence for the existence of nonfluorescent bodipy (4,4-difluoro-1,3,5,7-tetramethyl-4-bora-3a,4a-diaza-s-indacene) H dimers in double-labeled proteins and fluorescent J dimers in labeled lipid vesicles (Bergstrom, F.; et al. *J. Am. Chem. Soc.* **2002**, *124*, 196), allowing for the calculation of many of the properties of the dimers. Herein, we report on the use of molecular confinement within a sodium silicate derived glass to provide a highly reproducible system wherein nonfluorescent bodipy H dimers can be formed from the free probe essentially quantitatively without any interference from higher-order aggregates or fluorescent J dimers. The formation of the H dimer followed an unexpected first order kinetic process. On the basis of analysis of the fluorescence anisotropy of the entrapped monomer, it was concluded that the H-dimer formation was promoted by adsorption of monomers onto the silica surface (rate limiting step), followed by rapid dimerization. Using exciton coupling theory, it was determined that the H dimer consisted of two strongly coupled monomers that were stacked in a parallel orientation with a distance of 7.6 Å between the monomer units. The transition dipole moment of the monomer was determined to be 26.6×10^{-30} C m (8.1 D), the emission quantum yield of the H dimer was found to be close to zero, and the Förster distance for energy transfer between the monomer and H dimer was calculated to be 56 ± 2 Å. All of these values are in excellent agreement with those determined by Johansson et al.

Introduction

Bodipy fluorophores, which are based on 4,4-difluoro-1,3,5,7-tetramethyl-4-bora-3a,4a-diaza-s-indacene, have found increasing use as fluorescent probes in a number of applications, primarily owing to the large number of bodipy derivatives that are obtained upon modification of the probe at carbon positions 1, 3, 5, 7, and 8.[1] The commercial availability of bodipy derivatives for labeling proteins, oligonucleotides, dextrans, lipids, and polymer microspheres has rapidly extended their use to many areas in both life sciences and materials science. The attraction of bodipy-based probes arises from their visible excitation and emission wavelengths, high molar extinction coefficient, large quantum yield, good photostability, narrow emission bandwidth, the lack of ionic charge, which makes them insensitive to solvent pH, and the small change in dipole moment upon excitation, which renders them essentially insensitive to changes in dipolarity.

Recently, a number of applications of bodipy have been developed which take advantage of its property of being heavily autoquenched upon conjugation to proteins, primarily as a result of aggregation and/or dimerization between adjacent fluorophores.[2−4] Multiply labeled proteins release the monomeric form of the fluorophore upon proteolysis, resulting in a significant increase in fluorescence. This principle has been used in the analysis of protease activity[5−7] as well as in studies aimed at exploring distances between specific regions in proteins.[8−10] Very recently, the first experimental evidence for the existence of both fluorescent J dimers and nonfluorescent H dimers of bodipy has been provided using bodipy-labeled mutant forms of plasminogen activator inhibitor type 1 and bodipy-labeled lipids.[10] In the protein system, it was possible to generate a significant fraction of H dimers without interference from J dimers, and this allowed the photophysical properties of the H dimers to be calculated. However, this system was not capable of producing H dimers without a substantial fraction of monomer remaining, most likely because of proteins that were labeled with only a single fluorophore. Furthermore, this system required that derivatives of bodipy be used, thus there is no data at present concerning the formation of dimers by underivatized bodipy molecules.

In the present work, we describe a highly reproducible system that allows the quantitative formation of H dimers of bodipy based on molecular confinement of the dye within a sodium silicate derived glass. Molecular confinement has been examined extensively as a route to either prevent or promote aggregation/dimerization of fluorescent probes such as rhodamine and fluorescein.[11−17] For example, it has been extensively proven by López-Arbeloa's[11−14] and Levy's[15−17] groups that sol−gel derived materials provide a suitable support for the formation of either J dimers or H dimers of rhodamine, depending on the orientation of interacting monomers with respect to the adsorption surface. However, this is the first report on the use of molecular confinement to produce bodipy H dimers and, to our knowledge, is the only report of a system that is capable of promoting complete formation of nonfluorescent dimers with no interference from aggregates, unreacted monomers, or fluorescent J-dimer species. Insight into the mechanism of H-dimer formation within the silica matrix was obtained through a combination of fluorescence anisotropy measurements and kinetic studies of the dimer formation. These results show that the silica surface likely plays a direct role in the formation of the H dimer and may also shift the monomer−dimer equilibrium toward the formation of the dimer.

* To whom correspondence should be addressed. Phone: (905) 525-9140 (ext. 27033). Fax: (905) 527-9950. E-mail: brennanj@mcmaster.ca. Internet: http://www.chemistry.mcmaster.ca/faculty/brennan.

10.1021/jp027126y CCC: $22.00
Published on Web 11/22/2002

Using the dimer spectra obtained from this system, we were able to apply exciton coupling theory[18−20] to calculate several photophysical properties including the orientation, distance, and interaction energy of the monomer units within the dimer (which have not been previously reported), the transition dipole moment of the monomer, the absorptivity coefficient and emission quantum yield of the H dimer, and the Förster distance for energy transfer between the monomer and H dimer. These values are in good agreement with those obtained by Johansson et al.,[10] showing that the use of molecular confinement provides an excellent system for probing the properties of the H dimer. The determination of the intermonomer distance in the nonfluorescent dimer is important as it provides a means to calculate distances in multiply labeled proteins or biomolecular complexes. The energy transfer from the monomer to the dimer is also important as it is able to report on the evolution of sol−gel matrix, as demonstrated herein.

Experimental Section

Chemicals. Sodium silicate solution (technical grade, 9.1% sodium oxide, 29.2% amorphous silica, 61.7% water) was purchased from Fisher Scientific (Toronto, ON). Bodipy 505/515 (4,4-difluoro-1,3,5,7-tetramethyl-4-bora-3a,4a-diaza-s-indacene) was purchased from Molecular Probes (Eugene, Oregon). Dowex 50WX8-100 ion-exchange resin was purchased from Aldrich (Milwaukee, WI). Polymethacrylate fluorimeter cuvettes (transmittance curve C) were obtained from Sigma. Water was twice distilled and deionized to a specific resistance of 18 MΩ cm using a Milli-Q Synthesis A-10 water purification system. All other chemicals were of analytical grade and were used without further purification.

Preparation of Sol−Gel Derived Materials. Sodium silicate stock solutions were prepared using a procedure that was adopted from the work of Bhatia.[21] Briefly, 5.79 g of sodium silicate solution was dissolved in 20 mL of distilled water, the pH was adjusting to 4.0 by adding 7−10 g of Dowex 50WX8-100 ion-exchange resin, and the solution was then filtered through a 0.45 μm membrane filter and kept on ice to avoid polymerization. Stock solutions of bodipy (580 μM) in ethanol were used to prepare working solutions with bodipy concentrations in the range of 0.4−6.0 μM in ethanol (reference solution) and glycerol/water (0−100% (m/v) glycerol). The bodipy concentration was determined from its absorbance at 502 nm in ethanol ($\epsilon_{max} = 98\,000\ M^{-1}\ cm^{-1}$).[1] The absorbance spectra were measured immediately after sample preparation and then after selected time periods to assess the kinetics of dimer formation.

For the preparation of bodipy-doped sol−gel glasses, 1 mL of a solution containing 2.6 μM bodipy in water was mixed with 1 mL of the aqueous sodium silicate sol solution. The mixtures (final pH 6.3) were quickly poured into disposable polymethacrylate cuvettes which were sealed with Parafilm and left at 4 °C overnight to allow gelation to occur. Alternatively, 1 mL of the appropriate bodipy solution was diluted with 1 mL of distilled water to produce aqueous solutions containing 1.3 μM bodipy and only 0.2% (v/v) of ethanol. All samples were stored at 4 °C in the dark throughout the study.

UV−Visible and Steady-State Fluorescence Measurements. The absorption spectra of bodipy-doped silica glasses and the corresponding aqueous solutions were recorded with a Cary 400 UV−visible spectrophotometer (Varian Canada, Quebec) using undoped sol−gel samples or aqueous solutions as a blank. The same samples were used for fluorescence measurements, which were carried out at room temperature with a SLM 8100 spectrofluorimeter (Spectronic Instruments, Rochester, NY), as described previously.[15] Bodipy was excited at 488 nm with emission collected from 495 to 650 nm. All spectra were collected in 1 nm increments using 4 nm band-passes on the excitation and emission monochromators and an integration time of 0.3 s per point. Appropriate blanks were subtracted from each sample and the spectra were corrected for the wavelength dependence of the emission monochromator and photomultiplier tube.

Steady-state fluorescence anisotropy measurements were performed as described previously,[15] with excitation at 488 nm and emission at 515 nm. All fluorescence anisotropy values reported are the average of five measurements each on two different samples and were corrected for the instrumental G factor to account for any polarization bias in the monochromators.

Time-Resolved Fluorescence Measurements. Time-resolved fluorescence intensity data were acquired using an IBH 5000U time-correlated single photon counting fluorimeter, as described elsewhere.[15] Samples were excited with a pulsed light emitting diode operating at 1 MHz with a pulse duration of 1.3 ns and a wavelength of 495 nm. The LED was passed through a single grating monochromator (8 nm band-pass) set to 495 nm and then though a 500 nm short-pass filter. The intensity decay data was collected under magic angle polarization conditions, passed through a 505 nm long-pass filter and a single grating monochromator (16 nm band-pass) set to 515 nm, and was detected on a TBX-04 PMT detector. Intensity decay data was collected into 1024 channels (50 ps per channel) until 10 000 counts were obtained in the peak channel. The instrument response function was collected by measuring the Rayleigh scattering of the LED pulse from water (typical fwhm of 1.3 ns) and was used to deconvolute the instrument response profile from the experimentally determined decay trace. Appropriate time-shift parameters were obtained by allowing these to be floating parameters in the fit. All intensity decay data was fit to either single or double exponential decay models, with goodness of fit determined by the reduced chi-squared parameter ($\chi^2 < 1.10$) and the randomness of the residual plots.

Results and Discussion

Monomer−Dimer Equilibrium in Aqueous Solution. Absorption spectra were recorded at different time periods from solutions containing 0.9−6.0 μM bodipy in either pure water or in ethanol (where bodipy does not form dimers or aggregates[1]), with all samples stored at 4°C. Over the first 24 h after sample preparation, the absorbance of the aqueous bodipy solution decreased to a value of ∼0.06 AU for samples containing anywhere from 1.8 to 6 μM of the probe (supplementary data), with no new peaks appearing in the absorption spectrum of bodipy (Figure 1). The initial absorbance of the low and high concentration aqueous solutions was 2 or 10 times, respectively, lower than the corresponding value in ethanol. This indicates that a significant fraction of insoluble, nonabsorbing aggregates were present in aqueous solution at equilibrium. The observed difference between the absorption values of bodipy solutions in water and those in ethanol was drastically decreased upon addition of >25% glycerol to aqueous solutions, as a result of an increased solubility of bodipy in the presence of glycerol (Figure 2), confirming the presence of insoluble aggregates in aqueous bodipy solutions.

After 24 h, the absorption spectra of 0.4−1 μM bodipy solutions changed insignificantly, whereas the saturated solutions (≥3 μM) showed the slow growth of a new peak at 468 nm attributed to the bodipy H dimer (Figure 1). To our knowledge,

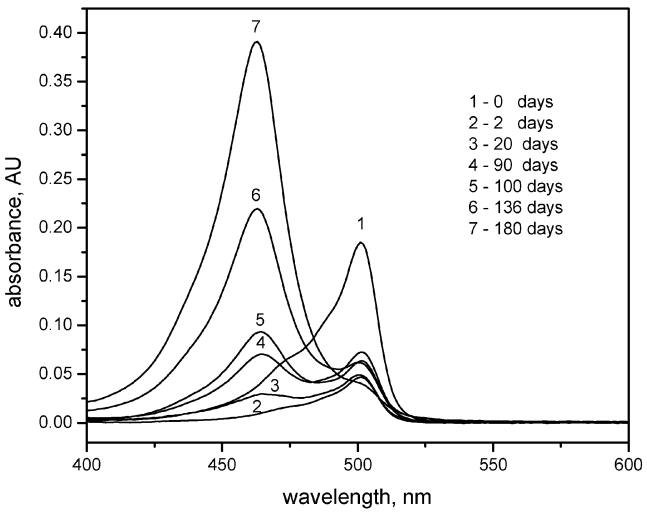

Figure 1. Changes in the absorption spectra of bodipy in water during storage at 4 °C. Bodipy concentration, 3.64 μM.

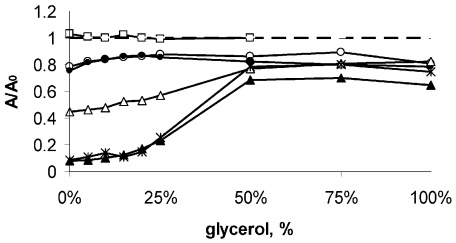

Figure 2. Ratios of absorbance values of bodipy in glycerol/water (A) and in ethanol (A_0). Samples were stored for 24 h at 4 °C after preparation. Bodipy concentration, 0.42 μM (○); 0.9 μM (●); 1.8 μM (△); 3.64 μM (▲); and 6 μM (*). Dashed line indicates the absorbance of bodipy in ethanol. Squares (□) indicate ratios of absorbance values of bodipy in glycerol-containing sodium silicate sol solution and in ethanol.

this is the first observation of bodipy H dimers in pure water. An important point to highlight is that the growth of the dimer occurred only after the monomer concentration had already diminished to approximately 25% of its initial value over the first 24 h of storage. After that, the monomer absorption remained essentially constant through the whole process of the dimer formation, with only minor increases in absorbance over 120 days, likely because of slow evaporation of solvent, and then decreased slowly after 180 days. The bodipy dimer was not formed in solutions containing either 25 mM Tris-HCl, pH 8.3 or glycerol at a level above 25%, at least over a period of 3 months. According to our data, glycerol shifts the monomer-aggregate equilibrium toward the monomer, whereas the presence of Tris ions shifts it toward the aggregate, by decreasing the solubility of bodipy in water.

The presence of aggregates as an intermediate species in the formation of dimers in solution is supported by the lack of an isosbestic point in the absorption spectra during the dimer formation, clearly indicating that a two-state equilibrium did not exist between the monomer and dimer. Furthermore, kinetic analysis of the loss of the monomer peak or the rise of the dimer peak did not follow either first or second order kinetics (kinetics were complex), negating the possibility of a simple reaction mechanism that did not involve intermediates. Finally, it should be noted that the changes in monomer absorbance exactly paralleled changes in fluorescence intensity (data not shown), but no changes were observed in the shape of the excitation spectrum, the fluorescence anisotropy, or the emission lifetime, consistent with the nonfluorescent nature of the H dimer and

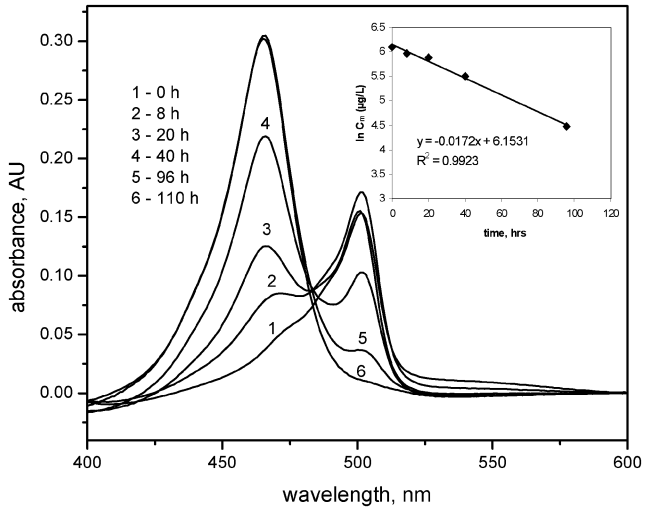

Figure 3. Dimerization of 1.65 μM bodipy in the aqueous sodium silicate sol−gel matrix at 4 °C. Sol−gel blocks were prepared by mixing equal parts of 2.6 μM bodipy solution in water and sodium silicate sol solution. Inset is linear plot of ln(c_m) versus time.

aggregate species, as proposed by Johansson.[10] Taken together, these data indicate that bodipy monomers rapidly aggregate in aqueous solution and then dimers slowly form from the aggregate over a period of several months. On the basis of the rate of dimer formation, it appears that one might expect to observe essentially pure dimer spectra after a sufficient time (>1 year) has elapsed to establish equilibrium in solution.

Bodipy Dimer Formation in Sodium Silicate Glass. The behavior of bodipy within sodium silicate derived glass was significantly different than that observed in solution. The most significant difference consisted of the lack of insoluble aggregates in the sol−gel system when bodipy was doped at the concentrations ≤2 μM. The absorption values of doped bodipy were as high as in ethanol and remained unchanged until the dimer peak started to appear in the absorption spectrum. This indicates that bodipy is initially present in the sol solution of silica in the monomeric form only.

Another important difference observed for entrapped bodipy relative to solution was the rapid appearance of the 468 nm H dimer peak only a few hours after sample preparation, and the rapid increase in dimer absorbance with a corresponding decrease in monomer absorbance, as shown in Figure 3. It is notable that the monomer−dimer equilibrium comes very close to moving through an isosbestic point, suggesting that the equilibrium predominantly involves two main species with almost no trace of an intermediate. Another notable difference relative to the solution results is that the dimerization proceeded until the monomer was essentially completely consumed, suggesting that the monomer−dimer equilibrium lies much farther to the right than in solution. On the basis of the loss of the monomer peak and the nonfluorescent nature of the probe at the completion of dimerization, it was calculated that less that 0.1% of the monomer remained at equilibrium, corresponding to an association constant for the monomer−dimer equilibrium of $>10^3$ (more than 100-fold greater than in solution).

To gain insight into the mechanism of the formation of dimers within sodium silicate glass, the kinetics of dimerization was examined by plotting the concentration of monomer remaining as a function of time. The loss of monomer was fit well to a first-order rate equation (see first-order plot inset in Figure 3) with a rate constant of 0.017 h^{-1} (4 °C). If the dimer had formed directly and essentially irreversibly from the monomer by the

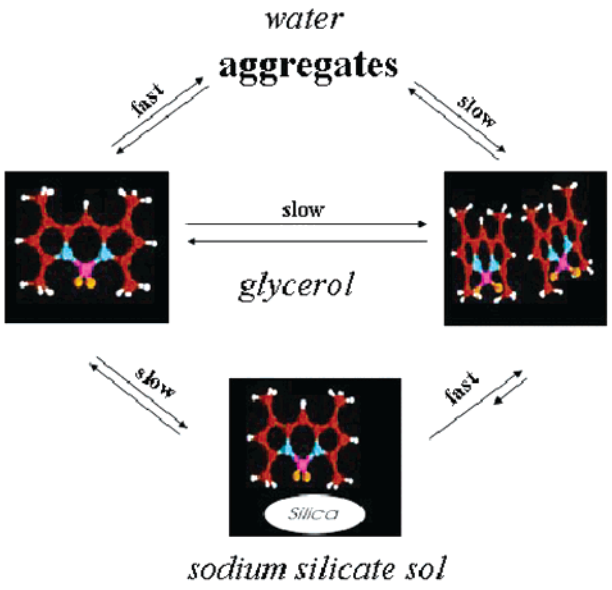

Figure 4. Scheme of different equilibria established in bodipy solutions in water, glycerol, and sodium silicate sol.

TABLE 1: Anisotropy of Bodipy in the Sodium Silicate Sol−Gel Matrix at the Different Levels of Dimerization. Bodipy Concentration, 1.3 μM[a]

physical state of the matrix	time, h	dimer conc, %	anisotropy
sol	0	0	0.0305 ± 0.0004
sol	10	5	0.0522 ± 0.0005
sol	20	12	0.0703 ± 0.0006
sol	40	40	0.1069 ± 0.0004
sol	96	78	0.1143 ± 0.0003
sol	110	> 99	0.1565 ± 0.0004
gel	150	> 99	0.1687 ± 0.0005

[a] Samples were kept at 4 °C.

reaction 2M → D, the rate of loss of the monomer would be expected to follow a second-order rate equation of the form $v = k[M]^2$. The loss of monomer by a first order process clearly shows that the dimer is not formed directly and points to a role for the sol−gel matrix in promoting the formation of dimer.

To assess the role of the silica matrix in bodipy dimerization, the rotational mobility of the monomer was assessed as a function of the percentage of dimer formed. As shown in Table 1, the anisotropy of bodipy increased slowly but steadily as the proportion of dimer increased, consistent with reduced mobility of the probe owing to adsorption onto the silica surface. Taken together, the anisotropy and kinetic data support the conclusion that the formation of dimers likely occurs directly from adsorbed monomers and that this intermediate dramatically increases both the rate and extent of dimerization relative to that in water. On the basis of the results of the kinetic analyses, the first order rate constant suggests a two step mechanism involving relatively slow adsorption of the monomer onto the surface (unimolecular process) followed by a more rapid dimerization step (Figure 4). Given that bodipy is not charged, it is possible that the conformation of the entrapped water, which is generally more highly structured than bulk water, may lower the solubility of the monomer and thus promote adsorption. Such a mechanism also explains the lack of aggregates within the glass, because the adsorption process would reduce the monomer concentration in solution and thus reduce the degree of aggregation.

A further insight into the mechanism of the dimerization was obtained by adjusting the rate of gelation of the sol. It was observed that bodipy dimerization proceeded with a similar efficiency and at essentially the same velocity in systems that gelled anywhere from a few minutes up to 6 h after addition of the probe. These results suggest that the probe adsorbs to the colloidal silica before gelation occurs, and that the matrix composition, rather than its physical state, control the solubility and aggregation properties of the doped bodipy.

TABLE 2: Photophysical Parameters of Bodipy Monomer and Dimer in the Sodium Silicate Sol−Gel Glass[a]

structure	λ_{abs}, nm	ϵ_{max}, M^{-1} cm^{-1}	ϕ_f	M_m, Cm	U, cm^{-1}	R, Å	α, °	θ, °
monomer	502	105 000	0.88	2.668×10^{-29}				
dimer	468	380 000	<0.0001		474	7.63	0	90

[a] λ_{abs}, absorption wavelength; ϵ_{max}, extinction coefficient; ϕ_f, fluorescence quantum yield; M_m, transition moment; U, interaction energy between monomers; R, intermonomeric distance; α, angle between the transition dipoles; θ, angle between the transition dipoles and the line joining the chromophore centers.

Calculation of Dimer Properties. Given that the entrapped bodipy system was able to provide essentially complete formation of the H dimer with no interference from aggregates, J dimers, or unreacted monomer, it was possible to use exciton theory to directly calculate many of the properties of the dimer. From the theory of exciton coupling within a pair of identical chromophores,[22,23] the ratio between the integrated absorption spectra of the dimer and the monomer is expected to be 2. We found that the ratio to be

$$\frac{\int \epsilon_d(\tilde{\nu})\tilde{\nu}^{-1}d\tilde{\nu}}{\int \epsilon_m(\tilde{\nu})\tilde{\nu}^{-1}d\tilde{\nu}} = 1.99 \qquad (1)$$

indicating that essentially full dimerization occurred for entrapped bodipy.

According to the exciton theory, the blue shift of the visible band of bodipy is typical of the formation of an H dimer in which the transition dipoles of the interacting bodipy molecules are parallel to each other and orthogonal to the line connecting the molecular centers of molecules. On the basis of the experimental absorption spectrum of the bodipy dimer in the sodium silicate derived glass, we calculated its photophysical parameters (Table 2). Because $\alpha = 0°$ and $\theta = 90°$, the distance between the molecular planes can be easily calculated from eq 2:

$$R^3 = \frac{M_m^{\,2}}{4\pi\epsilon_0 U} = 4.445 \times 10^{-28} m^3 \qquad (2)$$

which provides a distance of $R = 7.63$ Å. Also shown in Table 2 is the quantum yield for emission of the dimer, which indicates that the H dimer was essentially nonfluorescent, in agreement with the expectations of exciton coupling theory.[22]

The large blue shift and the vibrationless quality of the dimer band (Figure 5) resemble the so-called strong exciton coupling case of Simpson and Peterson.[24] In this model, criteria have been developed for two limiting cases (strong and weak coupling) in terms of the strength of the intermolecular interaction relative to the width of the absorption band for the individual molecule. In strong coupling, the splitting between the excited energy levels $2U$ is considered to be significantly greater than the Franck−Condon bandwidth ($\nu_{0-0} - \bar{\nu}$) of the corresponding electronic transition level in the monomer. According to our data, $\nu_{0-0} - \bar{\nu} = 413.1$ cm^{-1} and 1448 cm^{-1}/413.1 cm^{-1} = 3.51. Hence, the coupling of bodipy monomers

TABLE 3: Fluorescence Lifetimes (τ_1 and τ_2) of Bodipy in Solution and in Sol−Gel Glasses[a]

sample	medium	C_d, %	τ_1, ns	τ_2, ns
solution	25 mM Tris-HCl	0	5.85 ± 0.02	
	2.5 mM Tris-HCl	0	5.89 ± 0.03	
	water	0	5.81 ± 0.03	
	water	8	5.77 ± 0.03	
	water	12	5.74 ± 0.04	
	10% glycerol	15	5.81 ± 0.02	
sol solution	water	0	6.19 ± 0.03	
	water	15	6.17 ± 0.03	
	water	45	6.04 ± 0.02	
	water	90	5.85 ± 0.03	
gelled glass	water	>99	5.84 ± 0.04 (86%)	0.98 ± 0.04
	water (3 days of dry-aging)	>99	5.54 ± 0.02 (95%)	1.81 ± 0.02
	water (10 days of dry-aging)	>99	5.33 ± 0.02 (69%)	1.27 ± 0.02

[a] Dimer concentration (C_d) was calculated from the corresponding absorption spectra. Blank sol−gel samples showed no decay.

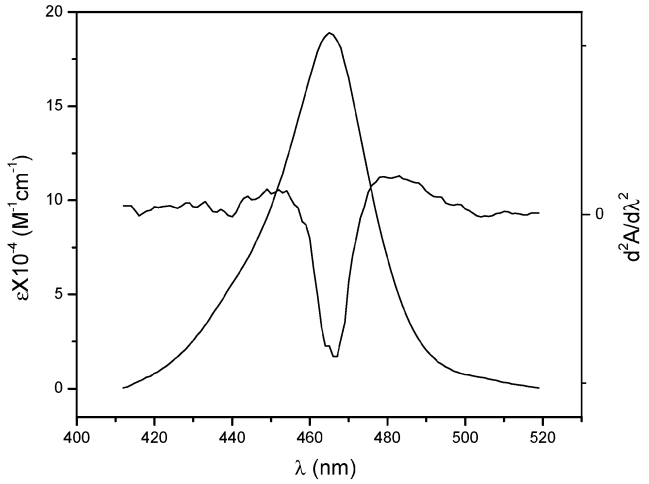

Figure 5. Calculated absorption spectrum and second derivative curve of the bodipy dimer.

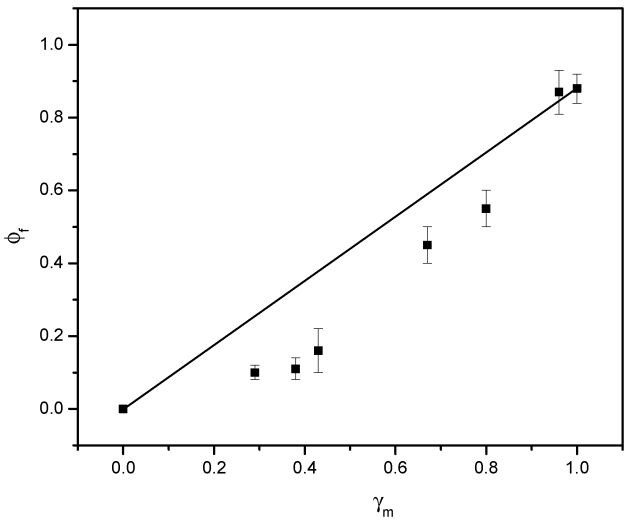

Figure 6. Fluorescence quantum yield (ϕ_f) versus γ_m. The λ_{ex}= 468 nm. The line corresponds to the case of ϕ_{fm} not quenched. (■): fit using eqs 8 and 10.

in the dimer structure is strong. Although the splitting suggests that two peaks should be present (one at higher and one at lower energy relative to the monomer peak),[24] the red-shifted peak is expected to have a vanishingly small intensity for the case where $\alpha = 0°$ and $\theta = 90°$ and, thus, is not observed in our spectra.

Fluorescence Properties of Entrapped Bodipy. Upon entrapment, the molecular confinement of a dye into nanometer sized cages can produce fluorescence behavior that is generally not observed in solution. To examine the behavior of the entrapped monomer, we examined both the emission intensity and the emission lifetime of the monomer as a function of the level of dimer present. The emission intensity of the entrapped bodipy (ϕ_f) relative to the fraction of light absorbed by the monomer (γ_m) should ideally be a linear relationship in the absence of factors such as quenching. However, as shown in Figure 6, the emission intensity shows a negative deviation from linearity, indicating that the monomer emission becomes partially quenched as the level of dimer increases.

The larger than expected decrease in the fluorescence emission intensity of bodipy at the onset of dimerization suggests that the loss of fluorescence intensity is related not only to the formation of the ground state dimer but was also affected by a secondary process involving quenching of monomer fluorescence. To confirm that dynamic quenching was present, the emission lifetime was measured as a function of dimer concentration. As shown in Table 3, the emission lifetime decreased by approximately 7% (from 6.2 to 5.8 ns) as the amount of dimer increased and decreased further as the glass aged, likely owing to decreases in pore sizes within the aging glass. Intriguingly, the onset of gelation also corresponds to the development of a second, short decay time (ca. 1 ns) that grows in proportion as the glass ages. The appearance of the second lifetime component for bodipy in the presence of dimers has been previously noted by Johansson,[9,10] and may be related to the effects of rapid energy transfer between molecules[25] or to the distribution of the dye in the aqueous phase and as adsorbates on colloidal particles.[26−29] Taken together, these data indicate that the monomer is quenched by a dynamic process which most likely involves energy transfer from the monomer to the dimer, as originally proposed by Johansson et al.[10]

A value for R_0 (distance of 50% efficiency for energy transfer) was determined according to eqs 3−5 using the bodipy dimer spectrum and the initial monomer emission spectrum obtained in the sol−gel glass:

$$R_0 = 9.79 \times 10^2(\kappa^2\Phi_0 J n^{-4})^{1/6}\ \text{nm} \qquad (3)$$

where κ is the orientation parameter ($\kappa^2 = 2/3$ for rotationally randomized orientation),[10] n is the refractive index of the bulk medium, and J is the integrated spectral overlap between the donor and acceptor which has been approximated by Campbell and Dwek[30] as

$$J = \sum F_d(\lambda)\, \epsilon_a(\lambda)\, \lambda^4\, \Delta\lambda \qquad (4)$$

where λ is wavelength in cm, $\epsilon_a(\lambda)$ is the absorptivity coefficient of the acceptor at λ, $\Delta\lambda$ is the wavelength increment (normally 1 nm or 10^{-7} cm), and $F_d(\lambda)$ is the fraction of the total

fluorescence intensity of the donor at λ normalized to the maximum absorptivity coefficient of the donor, as given by

$$F_d(\lambda) = \frac{F(\lambda)}{\sum F(\lambda)\Delta\lambda} \quad (5)$$

Using these equations, the value for R_0 was then determined to be 56 ± 2 Å with $\kappa^2 = 2/3$, $\Phi_0 = 0.88$, $n = 1.4$, and J calculated according to eq 4. This value is in excellent agreement with the value obtained by Johansson[10] and confirms that energy transfer between monomers and dimers occurs in the molecularly confined environment within a sol−gel derived glass. Using the calculated value of R_0 and the observed decrease in the emission lifetime, the average distance between monomers and dimers within the matrix was calculated to decrease from 90 to 62 Å. If it is assumed that both the monomer and dimer are adsorbed to the silica wall, the decrease in average distance is likely due to shrinkage of the pores as aging proceeded.[31] These results suggest that bodipy could be used to monitor changes in pore size for hydrated silica materials.

Conclusions

In the present work, we describe the dimerization of bodipy both in solution and when the dye is present in a sol−gel-derived matrix. In solution, the dimerization proceeds slowly via a nonfluorescent aggregate and does not go to completion. On the other hand, molecular confinement in a sol−gel-derived glass promotes rapid dimerization of bodipy with essentially no formation of higher-order aggregates or J dimers. The dimerization of entrapped bodipy is assisted by adsorption of the probe onto the surface of the silica, causing rapid dimerization relative to solution. On the basis of the experimental data and theoretical principles of exciton coupling, the bodipy dimer was determined to be formed from two strongly coupled monomers that were present in a parallel orientation with an intermonomer distance of 7.6 Å.

The described monomer-to-dimer transition of bodipy adds support to the well-established opinion that the formation of nonfluorescent aggregates or complexes is prevented in solid host materials, as a consequence of the isolation of the dye molecules from each other.[32,33,34] However, in the present system, dimer formation proceeds even before gelation of the sol has occurred, indicating that the silica surface, and not the pores, plays the critical role in dimer formation. The bodipy dye appears to be unique in that it is able to form H dimers almost completely owing to interactions with silica matrix. All other studies of dimer formation of dyes within sol−gel-derived materials indicate that H dimers generally exist along with a significant proportion of both monomer and J dimer species. The absence of higher-order aggregates and J dimers in bodipy-doped glasses suggests that monomer-to-dimer energy transfer may be used as a means of assessing the changes in pore morphology in hydrated silica systems.

Acknowledgment. The authors thank the Natural Sciences and Engineering Research Council of Canada, MDS-Sciex Inc., the Ontario Ministry of Energy, Science and Technology and the Canada Foundation for Innovation for funding this work. We also thank N. Janzen for technical assistance, Dr. F. Cortes for assistance in the modeling of the bodipy dimer conformation and the preparation of Figure 4, and Dr. F. Lopez-Arbeloa for helpful discussions. J.D.B. holds the Canada Research Chair in Bioanalytical Chemistry at McMaster University.

Supporting Information Available: Absorbance values of bodipy solution in glycerol water at 4 °C (Figure 1). This material is available free of charge via the Internet at http// pubs.acs.org.

References and Notes

(1) Haugland, R. P. *Handbook of Fluorescent Probes and Research Chemicals*, 6th ed; Molecular Probes: Eugene, OR, 1996.
(2) Jones, L. J.; Upson, R. H.; Haugland, R. P.; Panchuk-Voloshina, N.; Zhou, M.; Haugland, R. P. *Anal. Biochem.* **1997**, *251*, 144.
(3) Jiang, P.; Mellors, A. *Anal. Biochem.* **1998**, *259*, 8.
(4) Da Poian, A. T.; Gomes, A. M. O.; Coelho-Sampaio, T. *J. Virol. Methods* **1998**, *70*, 45.
(5) Thompson, V. F.; Saldana, S.; Cong, J.; Goll, D. E. *Anal. Biochem.* **2000**, *279*, 170.
(6) Jiang P.; Mellors, A. *Anal. Biochem.* **1998**, *259*, 8.
(7) Welder, F.; Moody, E.; Colyer, C. L. *Electrophoresis* **2002**, *23*, 1585.
(8) Karolin, J.; Fa, M.; Wilczynska, M.; Ny, T.; Johansson, L. B.-A. *Biophys. J.* **1998**, *74*, 11.
(9) Fa, M.; Bergstrom, F.; Haggloff, P.; Wilczynska, M.; Johansson, L. B.-A.; Ny, T. *Structure* **2000**, *8*, 397.
(10) Bergstrom, F.; Mikhalyov, I.; Hagglof, P.; Wortmann, R.; Ny, T.; Johansson, L. B.-A. *J. Am. Chem. Soc.* **2002**, *124*, 196.
(11) Ruiz-Ojeda, P. R.; Katime, I. A.; Ochoa, J. R.; López-Arbeloa, I. R. *J. Chem. Soc., Faraday Trans. 2* **1988**, *84*, 1.
(12) López-Arbeloa, F. L.; Ojeda, P. R.; López-Arbeloa, I. R. *Chem. Phys. Lett.* **1988**, *48*, 253.
(13) López-Arbeloa, F.; Martínez, V.; Bañuelos-Prieto, J.; López-Arbeloa, I. *Langmuir* **2002**, *18*, 2658.
(14) López-Arbeloa, F.; Herrán-Martínez, V.; López-Arbeloa, T.; López-Arbeloa, I. *Langmuir* **1998**, *14*, 4566.
(15) del Monte, F.; Levy, D. *J. Sol-Gel Sci. Technol.* **1997**, *8*, 585.
(16) Levy, D.; Ocaña, M.; Serna, C. J. *Langmuir* **1994**, *10*, 2683.
(17) del Monte, F.; Ferrer, M. L.; Levy, D. *Langmuir* **2001**, *17*, 4812.
(18) Fenkel, Y. I. *Phys. Rev.* **1931**, *37*, 17.
(19) Kasha, M. *Physical and Chemical Mechanisms in Molecular Radiation Biology*; Plenum: New York, 1991; p 231.
(20) Fidder, H.; Knoester, J.; Wiersma, D. A. *J. Chem. Phys.* **1991**, *95*, 7880.
(21) (a) Bhatia, R. B.; Brinker, C. J.; Ashley, C. S.; Harris, T. M. *Mater. Res. Soc. Symp. Proc.* **1998**, *519*, 183. (b) Bhatia, R. B.; Brinker, C. J.; Gupta, A. K.; Singh, A. K. *Chem. Mater.* **2000**, *12*, 2434.
(22) Kasha, M. *Radiat. Res.* **1963**, *20*, 55.
(23) Kasha, M.; Rawls, H. R.; El-Bayoumi, M. A. *Pure Appl. Chem.* **1965**, *11*, 371.
(24) Simpson, W. T.; Peterson, D. L. *J. Chem Phys.* **1957**, *26*, 588.
(25) Imhof, A.; Megens, M.; Engelberts, J. J.; de Lang, D. T.; Sprik, R.; Vos, W. L. *J. Phys. Chem. B* **1999**, *103*, 1408.
(26) Mishra, J. K.; Behera, P. K.; Parida, S. K.; Mishra, B. K. *Ind. J. Chem.* **1992**, *31B*, 118.
(27) Fassler, D.; Baezold, M. *J. Photochem. Photobiol. A*: *Chem.* **1992**, *64*, 359.
(28) Fassler, D.; Baezold, M.; Baexold, D. *J. Mol. Struct.* **1988**, *174*, 383.
(29) Levy, D.; Ocaña, M.; Serna, C. J. *Langmuir* **1994**, *10*, 2683.
(30) Campbell, I. D.; Dwek, R. A. *Biological Spectroscopy*; Benjamin/ Cummings Publishing Company Inc.: New York, 1984; pp 91−120.
(31) Black, I.; Birch, D. J. S.; Ward, D.; Leach, M. J. *J. Fluoresc.* **1997**, *7*, 111S.
(32) Avnir, D.; Kaufman, V. R.; Reisfeld, R. *J. Non-Cryst. Solids* **1985**, *74*, 395.
(33) McKiernan, J. M.; Yamanaka, S. A.; Dunn, B.; Zink, J. I. *J. Phys. Chem.* **1990**, *94*, 5652.
(34) Wehry, E. L.; Rogers, L. B. *Fluorescence and Phosphorescence Analysis*; Hercules, D. M., Ed.; Interscience: New York, 1966; pp 81−149.